Reversibility of the Hydrogen Desorption from $NaBH_4$ by Confinement in Nanoporous Carbon

Peter Ngene[a], Roy van den Berg[a], Margriet H. W. Verkuijlen[b], Krijn P. de Jong[a] and Petra E. de Jongh

Supplementary information

Effect of loading on the structure of the melt infiltrated nanocomposites

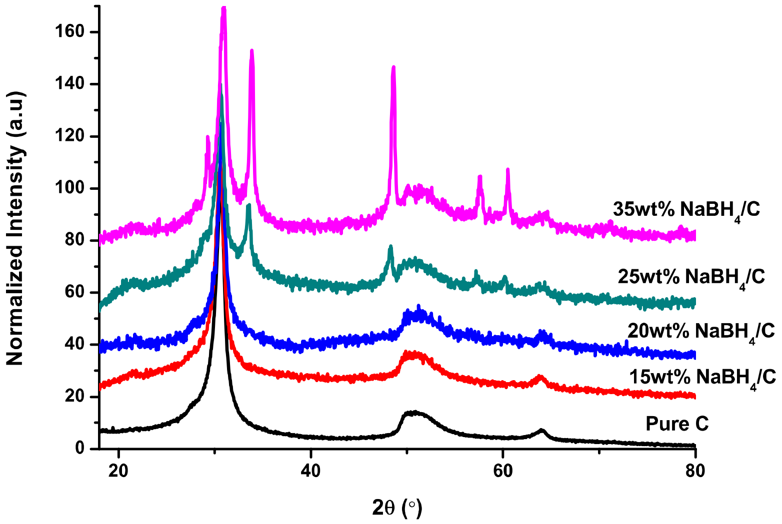

Fig. S1 XRD patterns of melt infiltrated $NaBH_4$/C nanocomposites with various loading of $NaBH_4$. No crystalline $NaBH_4$ is observed for composites containing less than 25wt% $NaBH_4$

Effect of $NaBH_4$ loading on the hydrogen release from the nanocomposites

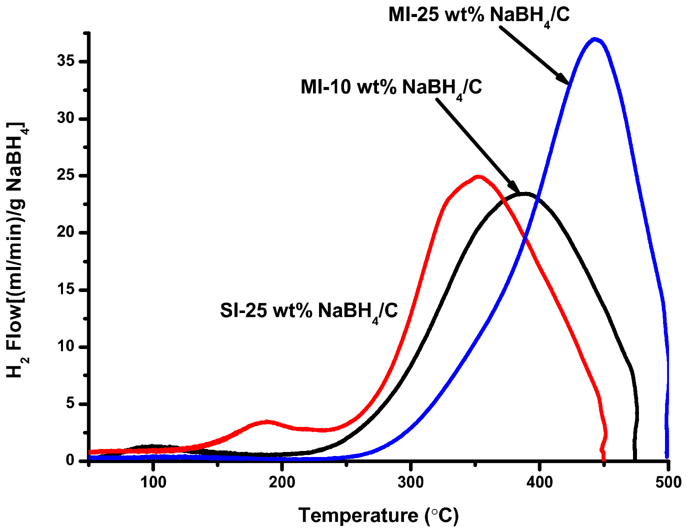

Fig.S2 Hydrogen release from 10 and 25 wt% melt infiltrated (MI) and 25wt% solution impregnated (SI) $NaBH_4$/C nanocomposites. For the MI samples, decreasing the $NaBH_4$ loading lead to desorption at lower temperatures which are comparable to the SI nanocomposite.

Cycling of the Nanocomposites

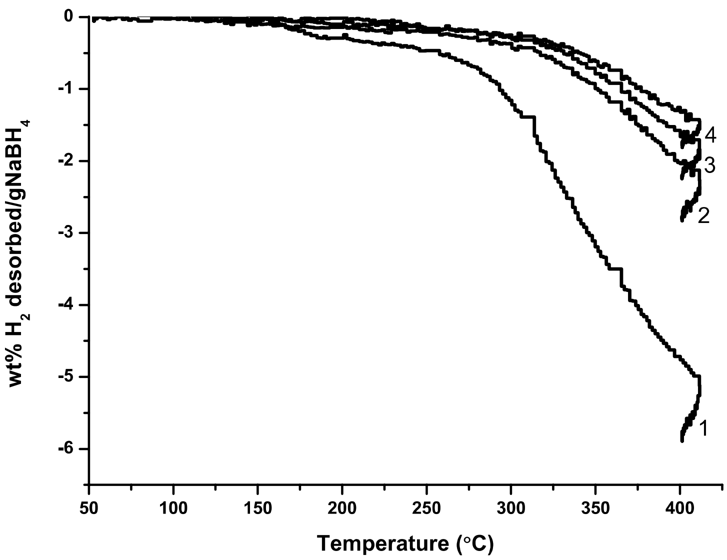

Fig.S3 Cycling (dehydrogenation and rehydrogenation cycles) of the nanocomposites as measured gravimetrically in Rubotherm suspension balance. The nanocomposites can be dehydrogenated and rehydrogenated (at 60 bar H_2, 325 °C for 5h) repeatedly. However, the capacity decreases upon cycling. Similar observation was made for the melt infiltrated nanocomposites.

Infiltration of carbon pores during dehydrogenation of physical mixtures

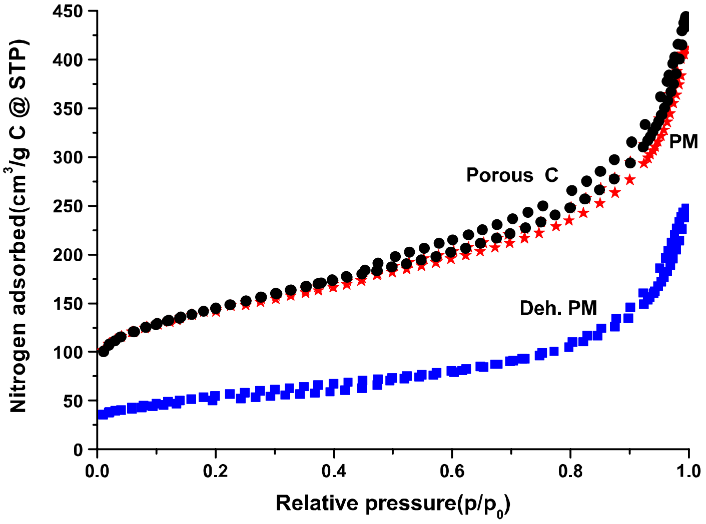

Fig.S4 Nitrogen physisorption showing a decrease in the volume of nitrogen adsorbed (decrease in pore volume of the carbon) after dehydrogenation of a physical mixture of 25wt% $NaBH_4$ and carbon. The total pore volume of the carbon decreased from 0.64 cm^3/g C for the physical mixture (PM) to 0.38 cm^3/g C after dehydrogenation (Deh. PM). This corresponds to a decrease of 0.26 cm^3/g C. The volume of $NaBH_4$ added in the mixture before desorption is 0.31 cm^3.

NMR of the dehydrogenated and rehydrogenated bulk $NaBH_4$

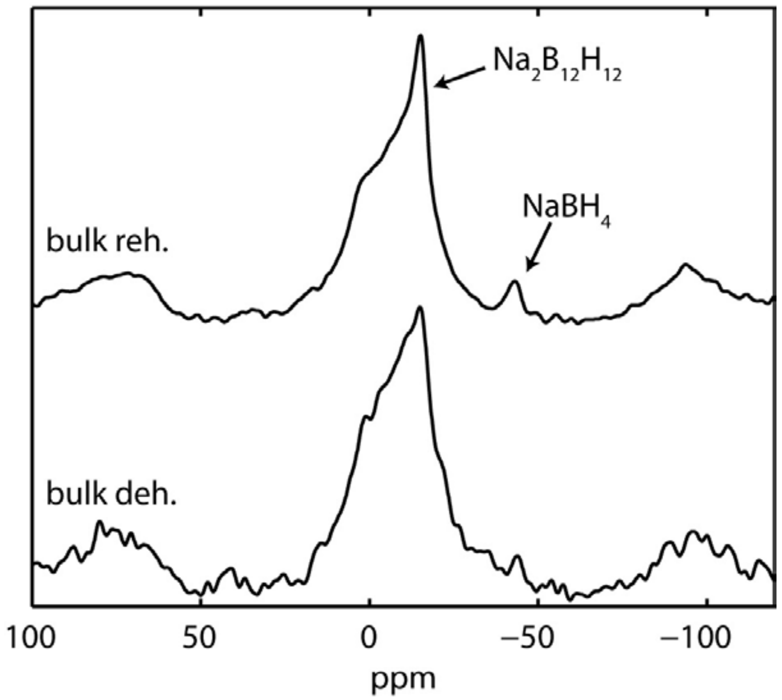

Fig.S5 Solid-state ^{11}B NMR spectra of dehydrogenated (bulk deh) and rehydrogenated (bulk reh) $NaBH_4$

The dehydrogenated $NaBH_4$ gives a broad peak mainly from amorphous $Na_2B_{12}H_{12}$ and traces of unreacted $NaBH_4$. After rehydrogenation at 60 bar H_2, 325 °C for 5 h, no major changes occurred in the structure of the compound, indicating no reversible formation of $NaBH_4$ during rehydrogenation

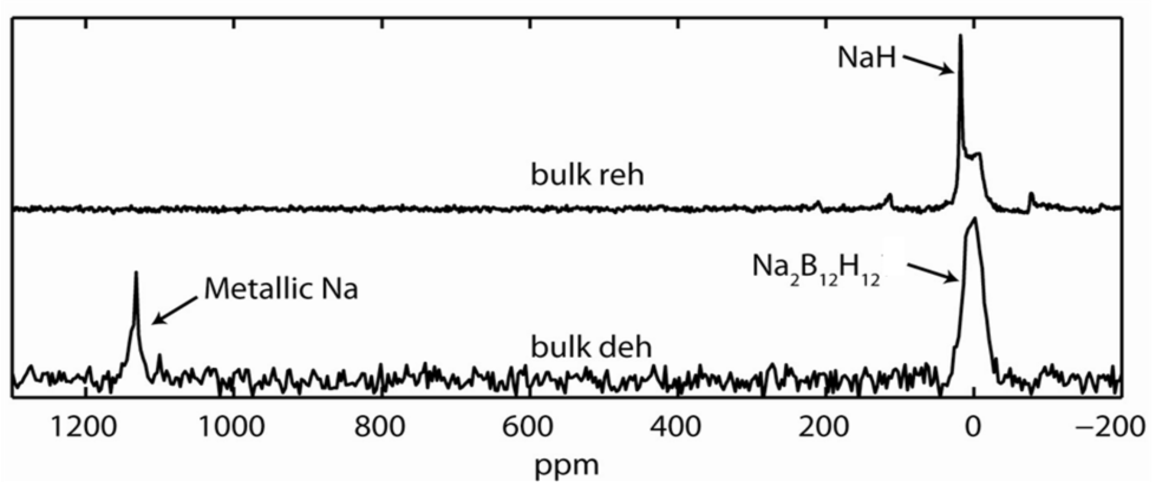

Fig.S6 Solid-state ^{23}Na NMR spectra of dehydrogenated (bulk deh) and rehydrogenated (bulk reh) $NaBH_4$

The dehydrogenated $NaBH_4$ gives resonances due to metallic Na and $Na_2B_{12}H_{12}$. After rehydrogenation, NaH peak is clearly seen, together with peak due to $Na_2B_{12}H_{12}$. The assignment of $Na_2B_{12}H_{12}$ in the ^{23}Na spectra is done based on the fact that large amount of $Na_2B_{12}H_{12}$ was also observed in the ^{11}B spectra (and not by a comparison with a ^{23}Na reference spectrum of $Na_2B_{12}H_{12}$). The resonance has a maximum at 3 ppm, and it is clearly not NaH which is at 18.3 ppm.

Equilibrium compositions for $NaBH_4$ decomposition

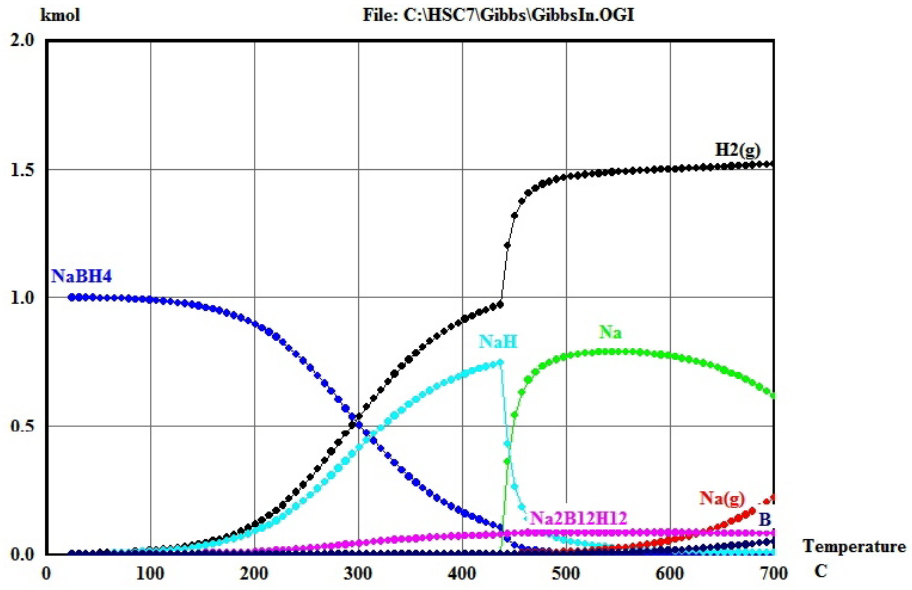

Fig.S7 Equilibrium diagram for the decomposition of $NaBH_4$. The calculation was done using HSC7 software and calculated standard enthalpy of formation of $Na_2B_{12}H_{12}$ in reference 54 of the main article.

The graph shows that Na and $Na_2B_{12}H_{12}$ are the thermodynamically most stable phases when $NaBH_4$ is heated to 600 °C. Note that only 1.5 mole H_2 (8.1 wt% H_2) per mole $NaBH_4$ is released while the Na formed is already in gaseous state above 450 °C, in line with the experimental results. Due to the high stability of $Na_2B_{12}H_{12}$, temperatures above 700 °C will be required for complete decomposition of $NaBH_4$ into Na and B.